THE JOURNAL OF BIOLOGICAL CHEMISTRY VOL. 289, NO. 43, pp. 29881–29891, October 24, 2014

Cardiomyocyte-specific Loss of Diacylglycerol Acyltransferase 1 (DGAT1) Reproduces the Abnormalities in Lipids Found in Severe Heart Failure*[S]

Received for publication, August 2, 2014, and in revised form, August 20, 2014 Published, JBC Papers in Press, August 25, 2014, DOI 10.1074/jbc.M114.601864

Li Liu[‡§1], Chad M. Trent[‡1,2], Xiang Fang[‡¶1,3], Ni-Huiping Son[‡], HongFeng Jiang[‡], William S. Blaner[‡], Yunying Hu[‡], Yu-Xin Yin[§4], Robert V. Farese, Jr.[‖], Shunichi Homma[**], Andrew V. Turnbull[‡‡], Jan W. Eriksson[‡‡§§], Shi-Lian Hu[¶], Henry N. Ginsberg[‡], Li-Shin Huang[‡], and Ira J. Goldberg[‡¶¶5]**

From the Divisions of [‡]Preventive Medicine and Nutrition and [**]Cardiology, Columbia University College of Physicians and Surgeons, New York, New York 10032, [§]Institute of Systems Biomedicine, Peking University Health Science Center, 100083 Beijing, China, [‖]Gladstone Institute of Cardiovascular Disease and Departments of Medicine and Biochemistry and Biophysics, University of California, San Francisco, California 94158, [¶]Department of Geriatrics, Affiliated Provincial Hospital, Anhui Medical University, 230001 Hefei, China, [‡‡]Astra-Zeneca Company, 431 50 Mölndal, Sweden, [§§]Department of Medical Sciences, Uppsala University, 751 05 Uppsala, Sweden, and [¶¶]Division of Endocrinology, Diabetes, and Metabolism, New York University Langone School of Medicine, New York, New York 10016

Background: Total body DGAT1 mice have no cardiac phenotype.
Results: Cardiomyocyte DGAT1 knock-out mice have increased mortality and accumulation of potentially toxic lipids, which were corrected by intestinal DGAT1 deletion and GLP-1 receptor agonists.
Conclusion: Cardiomyocyte DGAT1 deletion produces heart dysfunction and lipid abnormalities.
Significance: Lipotoxicity in the heart can be alleviated by changes in intestinal metabolism.

Diacylglycerol acyltransferase 1 (DGAT1) catalyzes the final step in triglyceride synthesis, the conversion of diacylglycerol (DAG) to triglyceride. *Dgat1*$^{-/-}$ mice exhibit a number of beneficial metabolic effects including reduced obesity and improved insulin sensitivity and no known cardiac dysfunction. In contrast, failing human hearts have severely reduced DGAT1 expression associated with accumulation of DAGs and ceramides. To test whether DGAT1 loss alone affects heart function, we created cardiomyocyte-specific DGAT1 knock-out (*hDgat1*$^{-/-}$) mice. *hDgat1*$^{-/-}$ mouse hearts had 95% increased DAG and 85% increased ceramides compared with floxed controls. 50% of these mice died by 9 months of age. The heart failure marker brain natriuretic peptide increased 5-fold in *hDgat1*$^{-/-}$ hearts, and fractional shortening (FS) was reduced. This was associated with increased expression of peroxisome proliferator-activated receptor α and cluster of differentiation 36. We crossed *hDgat1*$^{-/-}$ mice with previously described enterocyte-specific *Dgat1* knock-out mice (*hiDgat1*$^{-/-}$). This corrected the early mortality, improved FS, and reduced cardiac ceramide and DAG content. Treatment of *hDgat1*$^{-/-}$ mice with the glucagon-like peptide 1 receptor agonist exenatide also improved FS and reduced heart DAG and ceramide content. Increased fatty acid uptake into *hDgat1*$^{-/-}$ hearts was normalized by exenatide. Reduced activation of protein kinase Cα (PKCα), which is increased by DAG and ceramides, paralleled the reductions in these lipids. Our mouse studies show that loss of DGAT1 reproduces the lipid abnormalities seen in severe human heart failure.

All forms of heart failure are associated with derangements in lipid metabolism. In the setting of diabetes and obesity, it has been postulated that excess lipid accumulation in the heart leads to dysfunction, a condition referred to as lipotoxic cardiomyopathy (1, 2). Although in humans triglyceride (TG)[6] accumulation may be a marker (3, 4), experimental data in animal models have dissociated TG stores and heart dysfunction (5–7). Lipid accumulation also appears to worsen the response to ischemic injury (8). Despite a reduction in heart TG content, hearts from patients with severe heart failure had increased diacylglycerol (DAG) and ceramide content; the levels of these potentially toxic lipids decreased when heart function was improved via the use of left ventricular assist devices (9).

The heart obtains fatty acids both from the circulating pool of albumin-bound non-esterified fatty acids and from the very active hydrolysis of circulating lipoprotein-associated TGs (2).

* This work was supported, in whole or in part, by National Institutes of Health Grants HL45095 and HL73029 (to I. J. G.) from the NHLBI and Grant UL1 TR000040 from the National Center for Advancing Translational Sciences.
[S] This article contains supplemental methods and Tables 1 and 2.
[1] These authors contributed equally to this work.
[2] Supported by a predoctoral fellowship from the Heritage Affiliate of the American Heart Association.
[3] Supported by funds from Department of Human Resources and Social Security of Anhui Province and Anhui Provincial Hospital.
[4] Supported by the China National Major Scientific Program (973 Project 2010CB912202) and National Natural Science Foundation of China (Key Project 30930021).
[5] To whom correspondence should be addressed: Division of Endocrinology, Diabetes, and Metabolism; NYU Langone Medical Center; 522 First Ave., Smilow 9B, New York, NY 10016. Tel.: 646-501-0589; Fax: 212-263-9497; E-mail: Ira.Goldberg@nyumc.org.

[6] The abbreviations used are: TG, triglyceride; DAG, diacylglycerol; DGAT, diacylglycerol acyltransferase; FS, fractional shortening; PPAR, peroxisome proliferator-activated receptor; FFA, free fatty acid; GLP-1, glucagon-like peptide 1; CD36, cluster of differentiation 36; BNP, brain natriuretic peptide.

As in most tissues, fatty acids obtained in excess of those oxidized for energy are stored as TG in the heart. TGs are synthesized through the actions of diacylglycerol acyltransferases (DGATs), microsomal enzymes that catalyze the last step in the glycerol phosphate pathway, conversion of DAG to TG (10).

DGAT1 and DGAT2 are genetically distinct; both are expressed in the heart and have overlapping and distinct physiologic functions as genetic deletion of either leads to different phenotypes (11–13). DGAT1 knock-out mice fed a high fat diet are protected from diet-induced obesity and exhibit improved insulin resistance (14). A similar phenotype was noted when these mice were bred onto the Agouti background (15). Because DGAT1 inhibition reduces obesity, promotes insulin actions, and markedly reduces postprandial lipemia (16), DGAT1 inhibition might be beneficial in patients with obesity, type 2 diabetes mellitus, or severe hypertriglyceridemia leading to pancreatitis. This led to the development of a number of pharmacologic inhibitors (17) that reduce postprandial plasma TG (18–21) and decrease diet-induced obesity in rodents (17). These inhibitors also reduced post-prandial TG in a short term human study (22). However, DGAT1 inhibition might be expected to lead to accumulation of potentially harmful DAGs in the heart and other tissues.

Humans with severe heart failure have a marked reduction in DGAT1 mRNA levels in the heart, and this reduction in DGAT1 could be the reason for DAG and ceramide accumulation (9). Accumulation of DAGs and ceramides is associated with cellular and tissue dysfunction including defective insulin signaling (23), increased apoptosis (24), and activation of protein kinases (25). To test whether the lipid abnormalities observed in severe human heart failure were due to changes in DGAT1 expression, we deleted *Dgat1* in cardiomyocytes; these mice are denoted *hDgat1*$^{-/-}$. Loss of *Dgat1* in cardiomyocytes led to cardiomyopathy associated with accumulation of DAG and ceramides. We then performed experiments to correct this toxicity and found that enterocyte-specific deletion of DGAT1 (mice are denoted *hiDgat1*$^{-/-}$) corrected the cardiac dysfunction as did treatment with a long acting glucagon-like peptide 1 (GLP-1) receptor agonist, exenatide. These improvements were associated with reduced lipid uptake and decreased PKC activation in the hearts. Our data show that aberrant lipid metabolism found in human heart failure is a likely cause of further cardiac dysfunction. In addition, we show a possible new approach to treatment of lipotoxic diseases of the heart.

EXPERIMENTAL PROCEDURES

Mice and Diets—Animal protocols were in compliance with accepted standards of animal care and were approved by the Columbia University Institutional Animal Care and Use Committee and Peking University Health Center Animal Unit. Male and female mice were used in experiments unless specifically indicated. Wild-type (WT) C57BL/6J mice were purchased from The Jackson Laboratory. MHC-Cre mice were obtained from Michael Schneider (formerly at Baylor University) (26), and villin-Cre mice were obtained from The Jackson Laboratory. *Dgat1*$^{flox/flox}$ mice were generated as described (27). *hDgat1*$^{-/-}$ mice were generated by crossing MHC-Cre mice with *Dgat1*$^{flox/flox}$ animals. Heart and intestinal DGAT1 knock-out animals (*hiDgat1*$^{-/-}$) were from the mating of the *hDgat1*$^{-/-}$ mice with enterocyte-specific *Dgat1*$^{-/-}$ knock-out mice (16). Mice were housed in a barrier facility with 12-h light/12-h dark cycles and had *ad libitum* access to chow diet (5053 PicoLab Rodent Diet 20, Purina Mills).

DGAT Activity Assay Protocol—Heart DGAT activity was measured *in vitro* using membrane fractions isolated from muscle using [^{14}C]palmitoyl-CoA as described previously (28). Briefly, ventricular heart muscle was homogenized in buffer (20 mM HEPES, pH 7.4, 1 mM $CaCl_2$, 1 mM $MgCl_2$), 1 mM dithiothreitol, and a mixture of protease inhibitors containing phenylmethylsulfonyl fluoride, leupeptin, and pepstatin. One-fourth volume of 30% sucrose was added to the sample immediately following homogenization. The homogenization mixture was centrifuged at 1,500 × *g* for 10 min at 4 °C. The supernatant was spun at 150,000 × *g* for 1 h at 4 °C. The membrane pellet was homogenized and resuspended in buffer containing 20 mM HEPES, pH 7.4, 0.25 M sucrose, 1 mM dithiothreitol, and protease inhibitors. Protein concentration was determined using a protein assay reagent kit (Bio-Rad). DGAT1 activity in 10 μg of membrane protein was assayed using 200-μl reaction mixture containing 100 mM Tris, pH 7.5, 250 mM sucrose, 1 mg/ml bovine serum albumin, 150 mM $MgCl_2$, 0.8 mM EDTA, 0.25 mM 1,2-dioleoyl-*sn*-glycerol, and 25 μM [^{14}C]palmitoyl-CoA (0.3 μCi). The reaction was carried out at 37 °C for 5 min and stopped by lipid extraction, adding 0.75 ml of chloroform/methanol in a ratio of 2:1. After adding 0.375 ml of 1 mM H_2SO_4, 17 mM NaCl, the organic phase was removed and evaporated under a stream of N_2. Lipids were dissolved in 20 μl of hexane and then analyzed by TLC using plates that were developed in hexane/diethyl ether/glacial acetic acid in a ratio of 70:30:1 (v/v). Chromatographic bands containing TG were cut out after iodine staining and quantified by scintillation counting.

Exenatide and DGAT1 Inhibitor Treatment—Five- to 6-month-old male Dgat1$^{flox/flox}$ mice and *hDgat1*$^{-/-}$ mice were given saline or 40 μg/kg/day synthetic GLP-1 receptor agonist exenatide (Amylin Pharmaceuticals Inc.) injections subcutaneously twice daily for 4 weeks. DGAT1 inhibition studies were performed in 16-week-old male mice by oral gavage with 200 μl of vehicle (0.5% hydroxypropyl methylcellulose, 0.1% polysorbate 80) or 5 mg/kg DGAT1 inhibitor (AstraZeneca) upon food removal at 8 am as described (16). At 8-h postgavage, mice were euthanized, and tissues were collected for lipid measurement and RNA isolation.

Glucose and Fatty Acid Uptake—Sixteen-hour-fasted mice were first injected intravenously with 1 × 10^6 decays/min 2-deoxy-D-[^{3}H]glucose (PerkinElmer Life Sciences). Fifty-five minutes after 2-deoxy-D-[^{3}H]glucose injection, 1 × 10^6 decays/min [^{14}C]oleic acid complexed with 6% BSA was injected. Five minutes after oleic acid injection, blood was collected, and the vasculature was thoroughly perfused with 10 ml of PBS via cardiac puncture. Tissues were then excised, and accumulated radioactivity for [^{3}H]glucose and [^{14}C]oleic acid was measured via liquid scintillation counting. Data are expressed as the percentage of tissue counts/gram of tissue to plasma counts at 30 s (oleic acid) or 5 min (glucose).

Plasma Metabolites—Blood samples were obtained from 6-h-fasted mice. Glucose was measured directly from the tail tip with a glucometer (ONETOUCH Ultra 2, Lifescan, Inc.). Blood

was collected from the retro-orbital plexus for the measurement of plasma total cholesterol and TG. Plasma total cholesterol and TG were measured enzymatically using an Infinity kit (Thermo Electron Corp.).

Lipid Measurements—To measure free fatty acid (FFA), TG, DAG, and ceramide, lipids were extracted from left ventricular cardiac muscle with chloroform/methanol/HCl (v/v/v, 2:1:0.01) (29). Butylated hydroxytoluene (0.01%) was added in the extraction solution as an antioxidant, and [^{3}H]triolein (0.25 μCi) was used as an internal control for TG recovery. TG and FFA concentrations in lipid extracts were determined enzymatically with colorimetric kits (Sigma-Aldrich). DAG and ceramide levels were measured using a DAG kinase assay method (30). Basically, lipids from muscle samples were dried under a stream of N_2, redissolved in 7.5% octyl β-D-glucoside containing 5 mM cardiolipin and 1 mM diethylenetriamine pentaacetate in which DAG and ceramide are quantitatively phosphorylated to form ^{32}P-labeled phosphatidic acid and ceramide 1-phosphate, respectively, which were then quantified. The reaction was carried out at room temperature for 30 min in 100 mM imidazole HCl, 100 mM NaCl, 25 mM $MgCl_2$, 2 mM EGTA, pH 6.6, 2 mM DTT, 10 μg/100 μl DAG kinase (Sigma-Aldrich), 1 mM ATP, and 1 μCi/100 μl [γ-^{32}P]ATP. The reaction was stopped by addition of chloroform/methanol (v/v, 2:1) and 1% $HClO_4$, and lipids were extracted and washed twice with 1% $HClO_4$. Lipids were resolved by thin layer chromatography (TLC; Partisil K6 adsorption TLC plates, Whatman catalogue no. LK6D); the mobile phase contained chloroform/methanol/acetic acid (v/v/v, 65:15:5). The bands corresponding to phosphatidic acid and ceramide 1-phosphate were identified with known standards, and silicon was scraped into a scintillation vial for radioactivity measurement. [^{3}H]Triolein bands from the same TLC plates were identified and quantified in the same way and were used as controls for lipid recovery.

Electron Microscopy—Cardiac muscle from left ventricles from 16-h-fasted mice were isolated, fixed with 2.5% glutaraldehyde in 0.1 M Sorenson's buffer, pH 7.2, and treated with 1% OsO_4 also in Sorenson's buffer for 1 h. After dehydration and embedment in Lx-112 (Ladd Research Industries), thin sections (60 nm) were cut using a MT-7000 ultramicrotome, stained with uranyl acetate and lead citrate, and examined under a JEOL JEM-1200 EXII electron microscope. Pictures were taken by an ORCA-HR digital camera (Hamamatsu) and recorded with an Advanced Microscopy Techniques, Corp. Image Capture Engine.

Real Time PCR—Total RNA was isolated using a TRIzol kit from Invitrogen. One to 5 μg of RNA was initially treated with DNase I (Invitrogen). The RNA samples were then reverse transcribed using the SuperScript III First-Strand Synthesis System for RT-PCR. Real time amplification was performed using iQ SYBR Green Supermix (Bio-Rad). Primer sequences used for PCR amplification are listed in Table 1. Analysis was completed using iCycler iQ Real-Time Detection System software (Bio-Rad). Gene expression was normalized to β-actin mRNA levels.

Echocardiography—Two-dimensional echocardiography was performed using a high resolution imaging system with a 30-MHz imaging transducer (Vevo 770, VisualSonics) in unconscious mice. Before experiments, the mice were anesthetized with 1.5–2% isoflurane and thereafter maintained on 0.2–0.5% isoflurane throughout the experiment. Two-dimensional echocardiographic images were recorded in a digital format. Images were analyzed by a researcher blinded to the murine genotype. Left ventricular end diastolic dimension (LVIDd) and left ventricular end systolic dimension (LVIDs) were measured. The percentage of fractional shortening (FS) was calculated as follows: FS = ((LVIDd − LVIDs)/LVIDd) × 100.

TABLE 1
Primer sequences for RT-PCR analysis of gene expression

Primers	Forward	Reverse
Bactin	AGGCCCAGAGCAAGAGAGGTA	GGGGTGTTGAAGGTCTCAAACA
Plin2	CTACGACGACACCGAT	CATTGCGGAATACGGAG
Cidec	ATGCTGCAATGAAGACCGA	GCTAACCACTCTGGCACCAT
Plin5	TGAGGCAGAGCAAACACCGTAC	ATCCACTGCATTCTGCAGCTC
Ppara	TGCAGAGCAACCATCCAGA	ACCCGTTAATTAATGGCGAAT
Ppard	GCCTCGGGCTTCCACTAC	AGATCCGATCGCACTTCTCA
Pparg	GAGTGTGACGACAAGATTTG	GGTGGGCCAGAATGGCATCT
Atgl	CGCCTTGCTGAGAATCACCAT	AGTGAGTGGCTGGTGAAAGGT
Acox1	ATCACGGGCACTTATGC	TCTCACGGATAGGGACA
Pdk4	GACCGCTTAGTAACAC	GTAACGGGGTCCACTG
Cpt1b	GATGTTTGCAGAGCACGGCA	CCAGGTACCTGCTCACGGTA
Bnp	AGGTTTGCTATCTGGCA	ATGTCGAAGTTTAAGGCTCTGGA
Cd36	AATGGCACAGACGCAGCCT	GGTTGTCTGGATTCTGGA
Lpl	TCTGTACGGCACAGTGG	CCTCTCGATGACGAAGC
Glut4	AGAGTCTAAAGCGCCT	CCGAGACCAACGTGAA
Dgat1	GTGCACAAGTGGTGCATCAG	CAGTGGGATCTGAGCCATCA
Angptl4	GGAAAAGATGCACCCTTCAA	TGCTGGATCTTGCTGTTTTG

PKCα Activation Western Blotting—Heart tissue (20–30 mg) was homogenized in lysis buffer containing 20 mM HEPES, pH 7.4, 1 mM $CaCl_2$, 1 mM $MgCl_2$, 5 mM Na_3VO_4, 10 mM NaF, and 1 mM DTT with a mixture of protease inhibitors, and then ¼ volume of 30% sucrose was added to the samples immediately following homogenization. The mixtures were centrifuged at 1,500 × *g* for 10 min at 4 °C, and then the supernatants were collected and centrifuged at 150,000 × *g* for 1 h at 4 °C. The membrane pellets were homogenized and resuspended in 300 μl of buffer containing 20 mM HEPES, pH 7.4, 0.25 M sucrose, 5 mM Na_3VO_4, 10 mM NaF, 1 mM DTT, and protease inhibitors. The cytosolic fraction was obtained by concentrating the supernatants by acetone precipitation. 100 μg of protein of each sample was resolved by SDS-PAGE and transferred onto PVDF membranes. Immunoblotting was carried out using the primary antibody PKC-α. Integrin β1 and β-actin antibodies were used as membrane and cytosol controls (Abcam).

Statistics—All data are presented as mean ± S.D. unless indicated otherwise. Comparisons between two groups were performed using unpaired two-tailed Student's *t* test; comparisons of more than two groups were performed with one-way analysis of variance with Tukey's multiple comparisons test. Survival rates were analyzed with log rank test. A *p* value of less than 0.05 was used to determine statistical significance.

RESULTS

Phenotype of Heart-specific DGAT1 Knock-out Mice—Hearts from 3-month-old *hDgat1*$^{-/-}$ mice with cardiomyocyte-specific DGAT1 deletion had a marked reduction in DGAT1 mRNA (Fig. 1*A*). DGAT activity assays demonstrated that conversion of DAG to TG was reduced ~⅓ by loss of DGAT1 in cardiomyocytes, but this was not associated with a decrease in heart TG (Fig. 1*B*). DGAT1-deficient hearts had ~60% increased levels of total FFAs, 85% increased total DAG, and 95% increased total ceramide (Fig. 1*C*). There were no changes

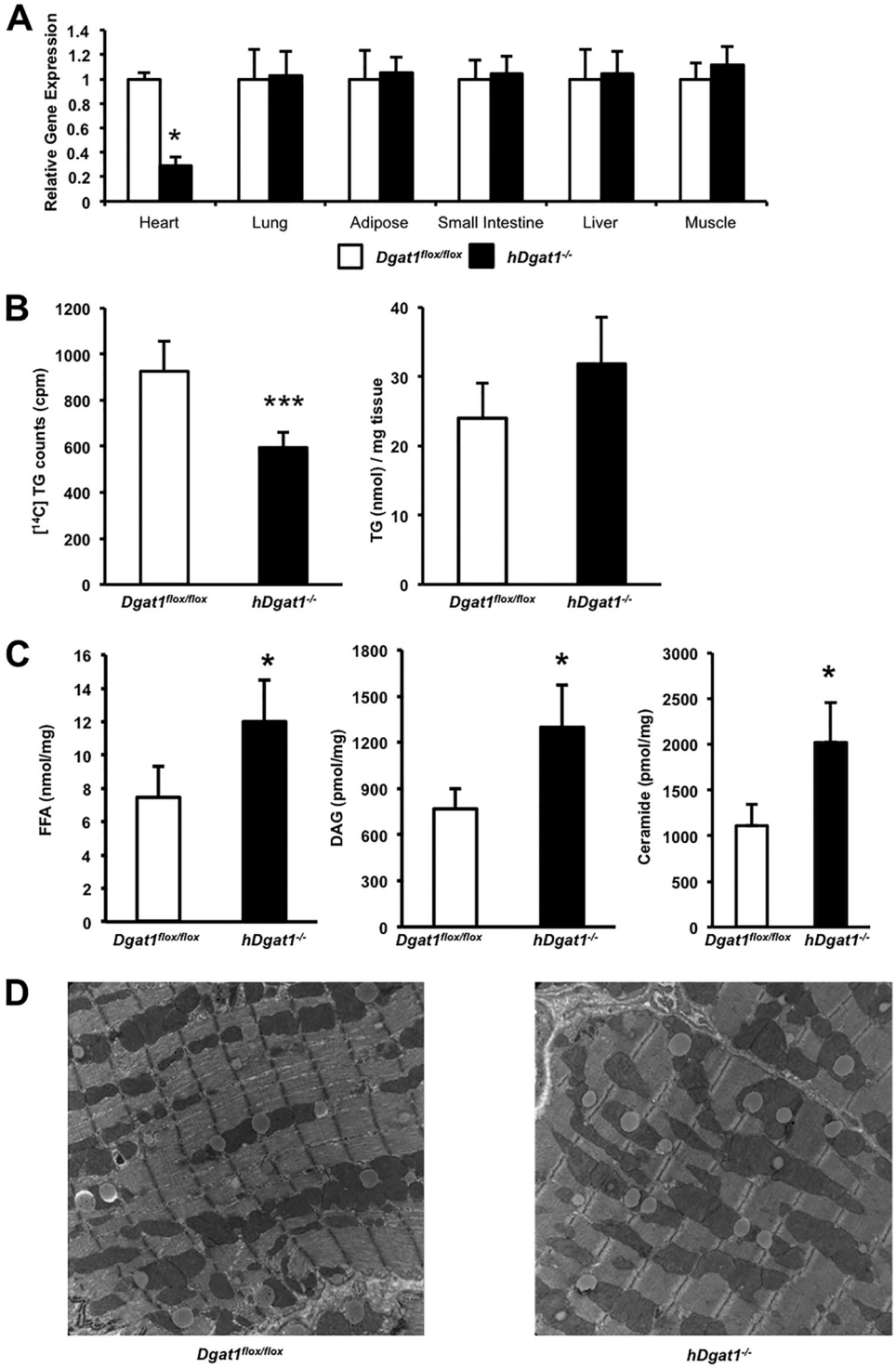

FIGURE 1. ***Dgat1* deletion in mouse cardiomyocytes.** *A*, tissue distribution of the DGAT1 mRNA levels in 3-month-old $Dgat1^{flox/flox}$ and $hDgat1^{-/-}$ mice measured by RT-PCR amplification ($n = 5$; *, $p < 0.05$). *B*, DGAT activity measured in 3-month-old $Dgat1^{flox/flox}$ and $hDgat1^{-/-}$ cardiac muscle ($n = 4–5$; ***, $p < 0.05$). *C*, heart FFA, DAG, and ceramide content from 3-month-old $Dgat1^{flox/flox}$ and $hDgat1^{-/-}$ mice ($n = 4–5$; *, $p < 0.05$). *D*, representative images of lipid droplets from 3-month-old $Dgat1^{flox/flox}$ and $hDgat1^{-/-}$ hearts. *Error bars* represent S.D.

in the circulating concentration of FFA, TG, glucose, or total cholesterol (Table 2). Both the number and size of lipid droplets, which accumulate after an overnight fast, did not change in 3-month-old $hDgat1^{-/-}$ mice (Fig. 1*D*).

As $hDgat1^{-/-}$ mice aged, they had reduced longevity compared with their control littermates (Fig. 2*A*). Curves for wild-type, $Dgat1^{flox/flox}$, and MHC-Cre transgenic mice were superimposable. Heart/body weight ratio was ~30% greater in 9-month-old $hDgat1^{-/-}$ mice (Fig. 2*B*). Although heart function was normal in young mice, older $hDgat1^{-/-}$ mice had a ~30% reduction in FS compared with $Dgat1^{flox/flox}$ control mice (Fig. 2*C*).

Cardiac Lipids in hDgat1$^{-/-}$ Hearts—Because total fatty acids and ceramides were increased, we measured individual lipid species with LC/MS. We observed an increase in total ceramides in hearts from *hDgat1*$^{-/-}$ mice (supplemental Table 1), although this increase was somewhat less than that found using the enzymatic method. C16, C18, C20, C20:1, C22:1, and C24:1 ceramides were significantly increased. Fatty acids were increased 75% in *hDgat1*$^{-/-}$ hearts due to an increase in C18, C18:1, and C18:2 fatty acids. There were no significant differences in other fatty acids or ceramides. In contrast, the only change in acyl-CoAs was a 26% reduction in C18 acyl-CoA.

TABLE 2

Plasma FFA, TG, glucose, and total cholesterol from 9-month-old Dgat1$^{flox/flox}$, hDgat1$^{-/-}$, and hiDgat1$^{-/-}$ mice (n = 4–5)

	Genotype		
	Dgat1$^{flox/flox}$	*hDgat1*$^{-/-}$	*hiDgat1*$^{-/-}$
FFA (nmol/ml)	315 ± 70.3	374.9 ± 101.3	185.8 ± 77.4[a]
TG (nmol/ml)	846.4 ± 163	854.0 ± 285.8	662.5 ± 302.7
Glucose (mM)	6.5 ± 0.4	7.1 ± 0.6	5.7 ± 0.4
Total cholesterol (pmol/ml)	700.6 ± 167.6	686.1 ± 217.4	490.6 ± 153.9

[a] $p < 0.05$.

Gene Expression Changes in hDgat1$^{-/-}$ *Hearts*—Consistent with the changes in heart function, the heart failure marker brain natriuretic peptide (*Bnp*) increased 5-fold in *hDgat1*$^{-/-}$ hearts (Table 3). In *hDgat1*$^{-/-}$ hearts, mRNA levels of *Ppara* increased ~50%, whereas *Pparg* decreased ~40%; *Ppard* did

TABLE 3

Gene expression in hearts from 3-month-old Dgat1$^{flox/flox}$ and hDgat1$^{-/-}$ mice (n = 5)

	Dgat1$^{flox/flox}$	*hDgat1*$^{-/-}$
Bnp	100 ± 44	563 ± 116[a]
Ppara	100 ± 29	150 ± 30
Ppard	100 ± 22	106 ± 12
Pparg	100 ± 16	58 ± 7[a]
Plin2	100 ± 39	173 ± 41[a]
Plin5	100 ± 46	64 ± 21
Cidec	100 ± 22	84 ± 32
Atgl	100 ± 21	87 ± 14
Cpt1b	100 ± 29	90 ± 22
Aox	100 ± 31	89 ± 23
Cd36	100 ± 25	141 ± 20[a]
Lpl	100 ± 28	125 ± 29
Angptl4	100 ± 26	73 ± 17
Pdk4	100 ± 24	62 ± 11
Glut4	100 ± 14	75 ± 5

[a] $p < 0.05$.

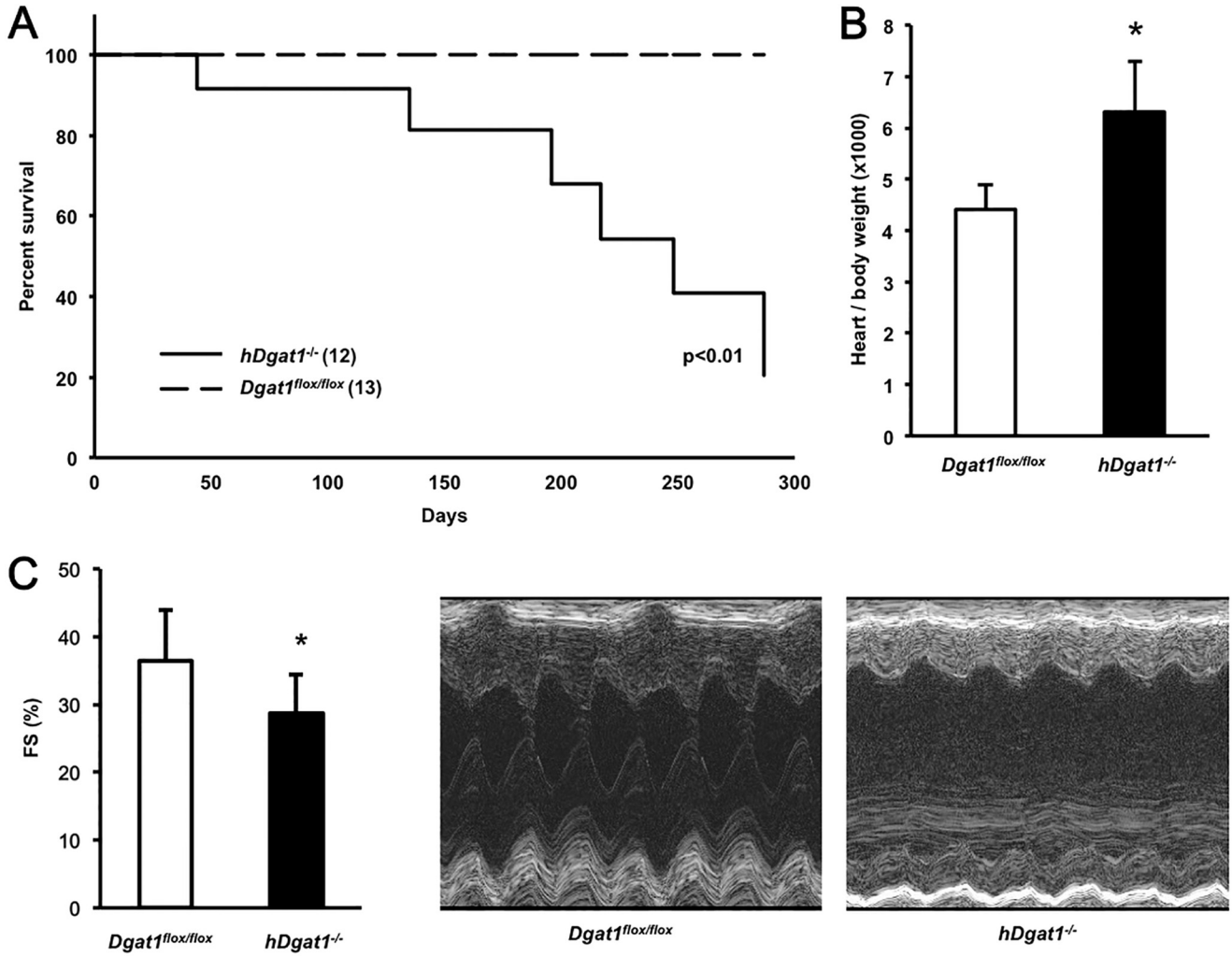

FIGURE 2. ***hDgat1*$^{-/-}$ knock-out mice have age-dependent death with heart failure.** *A*, *Dgat1*$^{flox/flox}$ and *hDgat1*$^{-/-}$ male mice were followed for 300 days, and the incidence of spontaneous death was recorded as a function of time (n = 12–13; *, $p < 0.01$). *B*, heart/body weight ratio in 9-month-old mice (n = 5–8; *, $p < 0.05$). *C*, fractional shortening measured with echocardiography in 9-month-old *Dgat1*$^{flox/flox}$ and *hDgat1*$^{-/-}$ mice (n = 4–5; *, $p < 0.05$). Representative M-mode echocardiography images are pictured. *Error bars* represent S.D.

not change significantly. Most genes affecting lipid droplet proteins were unchanged. Of the genes affecting lipid metabolism, mRNA levels of cluster of differentiation 36 (*Cd36*), a fatty acid transporter, increased ~40%. These gene changes are consistent with hearts having normal TG and lipid droplet production and an increase in TG precursors.

Intestinal and Heart DGAT1 Deletion—Our results showed that heart-specific deficiency of DGAT1 causes heart failure; these observations differed from those in *Dgat1*$^{-/-}$ mice that had normal cardiac function (6). We hypothesized that knock-out of DGAT1 in other tissues ameliorated the deleterious effects of cardiomyocyte DGAT1 deficiency. Recently, Lee *et al.* (33)reported that overexpression of DGAT1 in enterocytes negated the protection from insulin resistance reported in *Dgat1*$^{-/-}$ mice. Therefore, we tested whether knock-out of DGAT1 in the intestine would have beneficial effects in *hDgat1*$^{-/-}$ mice. We crossed *hDgat1*$^{-/-}$ mice with intestinal *Dgat1* knock-out (*iDgat1*$^{-/-}$) mice we created and described previously (16) to produce combined heart and intestinal knock-out (*hiDgat1*$^{-/-}$) mice. Intestinal loss of DGAT1 reduces intestinal motility and chylomicron production but leads to no cardiac phenotype (16). As we hypothesized, the survival rate for these double knock-out mice was improved (Fig. 3*A*). The increased heart/body weight ratio found in *hDgat1*$^{-/-}$ mice was normalized in double knock-out mice (Fig. 3*B*), and FS was improved by 40% (Fig. 3, *C* and *D*). The toxic lipids DAG and ceramide were reduced in the hearts of double knock-out mice (Fig. 3*E*).

Enterocyte-specific *Dgat1* deletion mice crossed onto the *hDgat1*$^{-/-}$ background had a number of changes in gene expression (Fig. 3*F*). Compared with *hDgat1*$^{-/-}$ mice, *hiDgat1*$^{-/-}$ mice had an ~50% reduction in *Bnp* mRNA and reduced *Ppara* expression but increased *Pparg* expression. *Cd36* expression was also reduced in *hiDgat1*$^{-/-}$ mouse hearts. Of note, on average, all PPARα target genes assessed (*Plin2*, *Atgl*, *Cpt1b*, *Aox*, *Pdk4*, and *Lpl*) were decreased.

Treatment of hDgat1$^{-/-}$ *Mice with Exenatide*—Intestinal knock-out of *Dgat1* increases circulating GLP-1 levels (16). For this reason, we tested whether GLP-1 receptor agonist treatment would also improve the cardiac toxicity found in the *hDgat1*$^{-/-}$ mice. We treated *hDgat1*$^{-/-}$ mice twice a day with 40 μg/kg subcutaneously injected exenatide for 1–4 weeks. Exenatide treatment of *hDgat1*$^{-/-}$ mice reduced the elevated cardiac DAG and ceramide levels (Fig. 4*A*). FS in exenatide-treated mice was also significantly improved (Fig. 4*B*, C). This treatment reduced *Bnp*, *Ppara*, and *Lpl* gene expression at 1 week of treatment and reduced *Cd36* gene expression after 4 weeks of treatment (Fig. 4*D*), but mRNA levels of genes mediating fatty acid oxidation did not change (other genes are shown in Table 4). Total DAG and ceramide levels decreased (Fig. 4*E*); the ceramide reduction was due to lesser C16, C18, C24, and C24:1 ceramides (supplemental Table 2).

We then tested whether the toxicity due to cardiomyocyte DGAT1 deletion affected FFA uptake and whether exenatide treatment corrected any abnormalities. *hDgat1*$^{-/-}$ mouse hearts had greater uptake of FFA than control littermates. Exenatide treatment normalized uptake of labeled oleic acid by the *hDgat1*$^{-/-}$ hearts (Fig. 5*A*) and increased heart uptake of 2-deoxyglucose (Fig. 5*A*). One week of exenatide also decreased serum glucose and FFA concentrations. FFA decreased from 375 $\pm$ 101 to 199 $\pm$ 79 nmol/ml, TG decreased from 854 $\pm$ 286 to 724 $\pm$ 317 nmol/ml, and glucose decreased from 7.1 $\pm$ 0.5 to 5.8 $\pm$ 0.5 mM (all significant $p < 0.5$); the cholesterol decrease from 696 $\pm$ 217 to 548 $\pm$ 184 was not significant ($n = 5$). Therefore, exenatide likely corrected the abnormalities in toxic lipid accumulation by reducing heart lipid uptake.

PKC Activation and Correction—Alterations in the accumulation of intracellular toxic lipids are likely to affect a number of downstream pathways. In previous work, we showed that cardiac PKCs were activated in hearts from mice with excess lipid accumulation (34). Membrane association of PKCα, which indicates activation, was increased 6-fold in hearts from *hDgat1*$^{-/-}$ mice (Fig. 5*B*); *iDgat1*$^{-/-}$ hearts were similar to control. This increase was reduced by about half with intestinal *Dgat1* deletion or exenatide treatment (Fig. 5, *B* and *C*).

DGAT1 Inhibition—We and others have shown previously that pharmacologic DGAT1 inhibition increases circulating GLP-1 levels in mice (16, 35). To determine whether this would lead to changes in heart gene expression, a single dose of a pharmacologic DGAT1 inhibitor was given to fasting mice, and hearts were harvested 8 h later. *Ppara* was modestly decreased. *Ppard* and *Pparg* did not change. *Ppara* target genes *Pdk4*, *Cpt1b*, and *Lpl* were not changed, but *Cd36* mRNA levels were reduced 25% (Table 5). This acute single dose did not reduce heart TG or FFA.

DISCUSSION

We tested whether reduced DGAT1 expression could be responsible for lipid abnormalities observed in the hearts of humans with severe heart failure. By producing cardiomyocyte-specific *Dgat1* knock-out mice, we created a lipid phenotype that was the opposite of heart-specific *Dgat1* overexpression (5, 7) and reproduced many of the features found in human heart failure, *i.e.* increased DAG and ceramide levels. These lipid increases were unlike those found in hearts from total body *Dgat1*$^{-/-}$ mice (14) and from studies using pharmacologic DGAT1 inhibitors (36). *hDgat1*$^{-/-}$ mice died prematurely with cardiac hypertrophy and heart failure. The elevated DAG and ceramide levels are the biochemical result that would be predicted upon loss of DGAT1 (37). Heart failure was documented by reduced FS and increased heart expression of BNP. Although not specifically studied in these mice, cardiac lipotoxicity in a previous mouse model led to sudden death from ventricular fibrillation (38).

Dgat1$^{-/-}$ mice do not have heart dysfunction (6). They are resistant to high fat diet-induced insulin resistance and obesity and have extended longevity (14, 39). *Dgat1*$^{-/-}$ mice also have increased whole body energy expenditure associated with increased locomotor activity (14, 15, 40). This beneficial phenotype was initially thought to be due to increased levels of adiponectin (41); however, the effects were reversed by enterocyte-specific DGAT1 overexpression (33). *iDgat1*$^{-/-}$ mice, like total body *Dgat1*$^{-/-}$ mice, have delayed gastric emptying, diminished chylomicron secretion, and increased plasma levels of GLP-1 (16). When we crossed *hDgat1*$^{-/-}$ mice with *iDgat1*$^{-/-}$ mice to create *hiDgat1*$^{-/-}$ mice, heart function and survival improved compared with *hDgat1*$^{-/-}$ mice. Thus, the

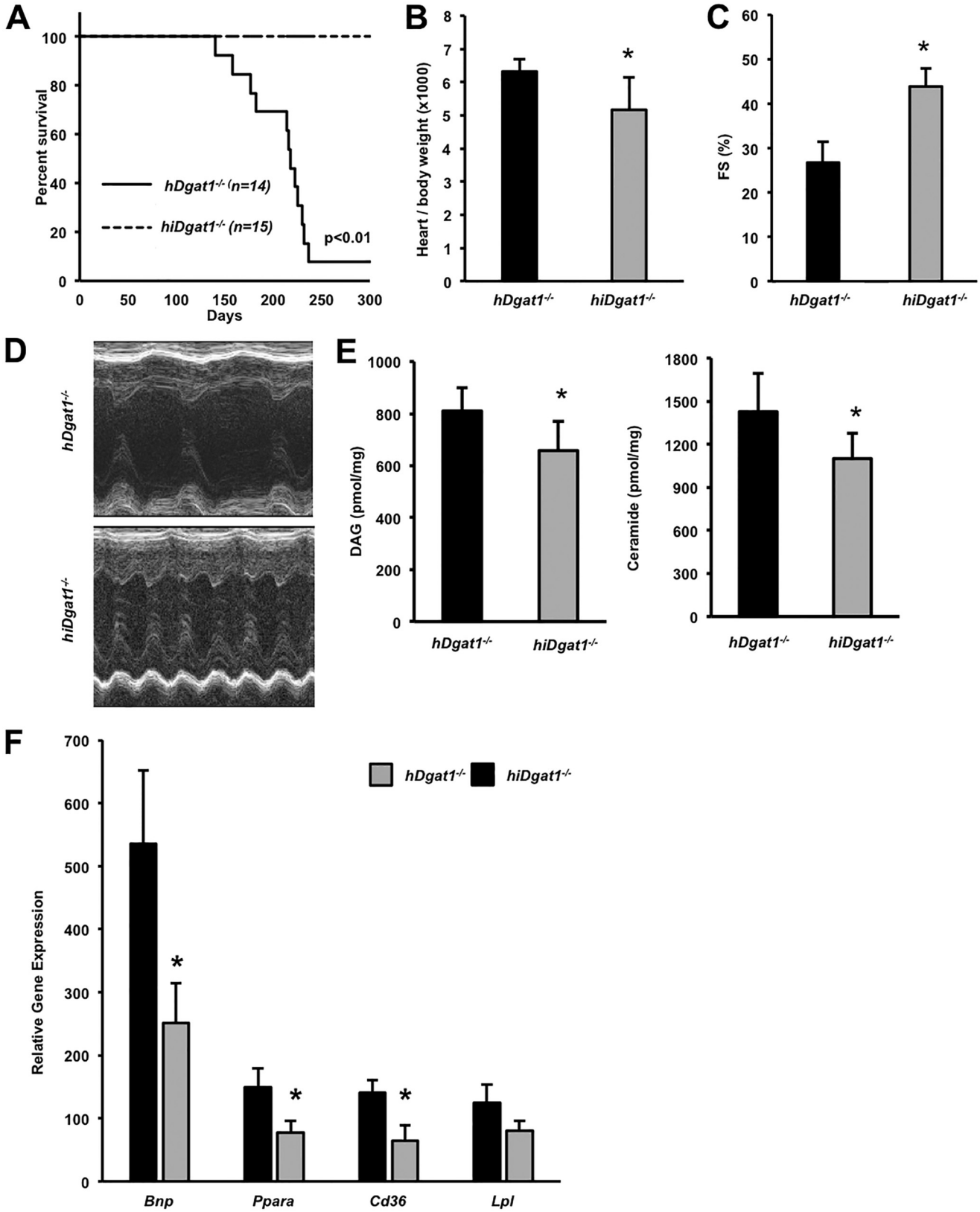

FIGURE 3. **Intestinal DGAT1 deletion ameliorates heart failure of *hDgat1*$^{-/-}$ mice.** *A*, male and female *hDgat1*$^{-/-}$ and *hiDgat1*$^{-/-}$ mice were followed for 300 days, and the incidence of spontaneous death was recorded as a function of time ($n = 14–15$; *, $p < 0.01$). *B*, heart/body weight ratio in 9-month-old mice *hDgat1*$^{-/-}$ and *hiDgat1*$^{-/-}$ mice ($n = 5$; *, $p < 0.05$). *C*, fractional shortening was measured with echocardiography in 9-month-old *hDgat1*$^{-/-}$ and *hiDgat1*$^{-/-}$ mice ($n = 5$; *, $p < 0.01$). *D*, representative M-mode echocardiography images are shown. *E*, DAG and ceramides were measured in hearts of 9-month-old *hDgat1*$^{-/-}$ and *hiDgat1*$^{-/-}$ mice ($n = 5$; *, $p < 0.05$). *F*, mRNA levels of *Bnp*, *Ppara*, *Cd36*, and *Lpl* in hearts from 9-month-old *hDgat1*$^{-/-}$ and *hiDgat1*$^{-/-}$ mice ($n = 6$; *, $p < 0.05$). *Error bars* represent S.D.

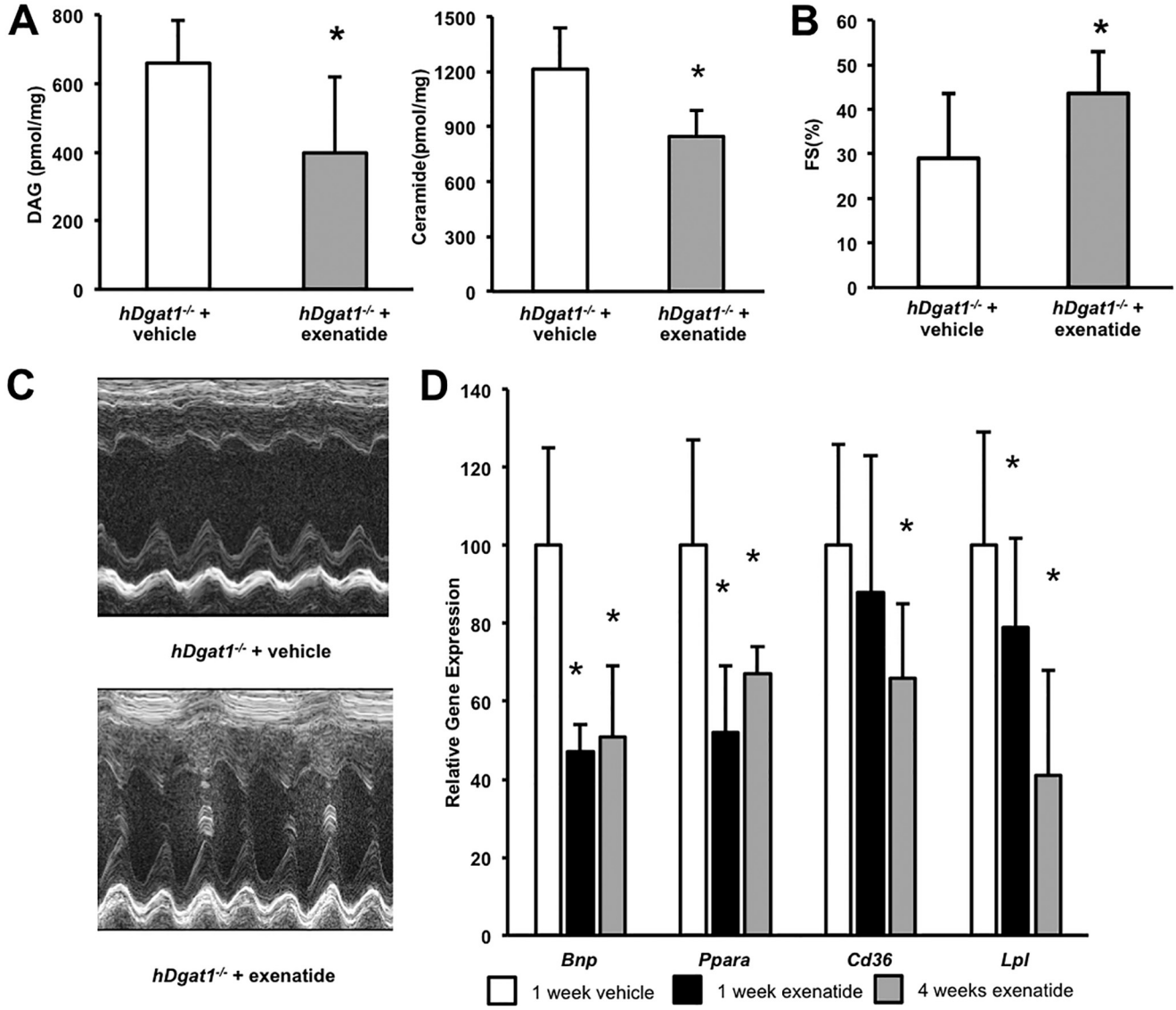

FIGURE 4. **Treatment of *hDgat1*$^{-/-}$ mice with exenatide improved heart function.** *A*, DAG and ceramides were measured in hearts from 5–6-month-old vehicle- and exenatide-treated *hDgat1*$^{-/-}$ mice ($n = 5$; *, $p < 0.05$). *B*, fractional shortening in 5–6-month-old vehicle- and exenatide-treated *hDgat1*$^{-/-}$ mice ($n = 6$–7; *, $p < 0.05$ *versus hDgat1*$^{-/-}$) (*right panel*). *C*, representative M-mode echocardiography images are shown. *D*, mRNA levels of *Bnp*, *Ppara*, *Cd36*, and *Lpl* in hearts from 5–6-month-old *hiDgat1*$^{-/-}$ mice treated with vehicle, exenatide for 1 week, and exenatide for 4 weeks ($n = 6$; *, $p < 0.05$). *Error bars* represent S.D.

TABLE 4

Gene expression in hearts from 5–6-month-old vehicle- or exenatide-treated hDgat1$^{-/-}$ mice ($n = 7$)

	hDgat1$^{-/-}$ + vehicle	*hDgat1*$^{-/-}$ + exenatide
Bnp	100 ± 20	51 ± 18[a]
Ppara	100 ± 30	74 ± 6
Ppard	100 ± 44	90 ± 56
Pparg	100 ± 10	126 ± 25[a]
Plin2	100 ± 18	75 ± 16[a]
Plin5	100 ± 29	91 ± 26
Cidec	100 ± 41	94 ± 37
Atgl	100 ± 16	63 ± 18[a]
Cpt1b	100 ± 40.8	106 ± 38
Aox	100 ± 33	110 ± 23
Cd36	100 ± 29	66 ± 19[a]
Lpl	100 ± 37	41 ± 27[a]
Angptl4	100 ± 27	153 ± 45[a]
Pdk4	100 ± 33	151 ± 29[a]
Glut4	100 ± 18	56 ± 17[a]

[a] $p < 0.05$ *versus hDgat1*$^{-/-}$ + vehicle.

deleterious effects of *Dgat1* deletion in the heart were reversed by intestinal DGAT1 deficiency. One option for the beneficial actions of intestinal DGAT1 deficiency is that the marked defect in early chylomicron formation shielded the hearts from dietary fat accumulation (16). Another option is that increased GLP-1 altered heart lipid metabolism. Treatment of *hDgat1*$^{-/-}$ mice with exenatide reduced *Bnp* mRNA, evidence that pathological cardiac stress was improved in *hDgat1*$^{-/-}$ mice. DAG and ceramide were also reduced in exenatide-treated *hDgat1*$^{-/-}$ mouse hearts. These metabolic changes were associated with an improvement in cardiac function as measured by FS.

Examination of gene expression and heart lipid content supported the hypothesis that the heart dysfunction and its amelioration were due to changes in metabolism. Exenatide treatment of *hDgat1*$^{-/-}$ mice reduced mRNA levels of the lipid uptake genes *Cd36* and *Lpl*. We then showed that the reduction in heart lipids

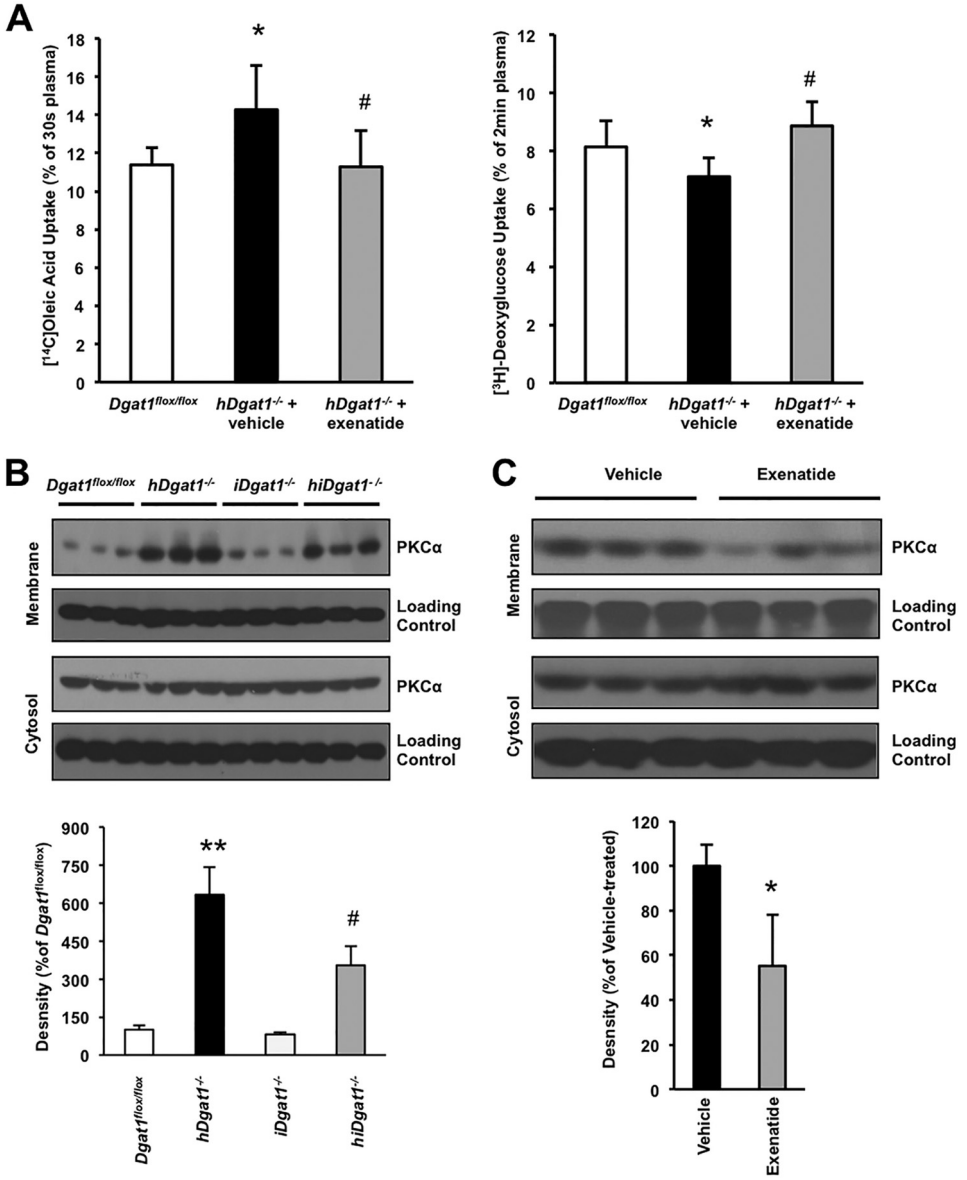

FIGURE 5. **Fatty acid and glucose uptake and PKC activation.** *A*, heart fatty acid and glucose uptake were measured in 5–6-month-old vehicle- or exenatide-treated *hDgat1*$^{-/-}$ mice ($n = 9$–11; *, $p < 0.05$ *versus Dgat1* $^{flox/flox}$; #, $p < 0.05$ *versus hDgat1*$^{-/-}$ + vehicle). *B*, PKCα activation was measured by Western blotting in 5–6-month-old *Dgat1* $^{flox/flox}$, *hDgat1*$^{-/-}$, *iDgat1*$^{-/-}$, and *hiDgat1*$^{-/-}$ hearts. Representative blots for membrane and cytosolic fractions (*upper panel*) and density difference (*lower panel*; **, $p < 0.01$ *versus Dgat1*$^{flox/flox}$; #, $p < 0.05$ *versus hDgat1*$^{-/-}$) are shown. *C*, PKCα activation was measured by Western blotting in hearts from 5–6-month-old vehicle- and exenatide-treated *hDgat1*$^{-/-}$ mice. Representative blots for membrane and cytosolic fractions (*upper panel*) and density difference (*lower panel*; $n = 3$; *, $p < 0.05$ *versus hDgat1*$^{-/-}$ + vehicle) are shown. *Error bars* represent S.D.

was associated with reduced *in vivo* uptake of fatty acids. Because plasma fatty acid levels were also reduced by exenatide, the tracer kinetic studies alone underestimate the total decrease in heart fatty acid accumulation. It is likely that reduced lipid uptake prevented cardiac toxicity and accounted for the beneficial effects of GLP-1 agonist treatment in obesity-driven cardiomyopathy models (42). Although GLP-1 receptor agonists improve heart function, it is not likely that defective GLP-1 signaling alone is the cause of lipotoxicity as mice with a cardiomyocyte deletion of the GLP-1 receptor have no heart phenotype (43).

How do these changes in lipid metabolism alter heart function? Many pathways are likely to be activated in the setting of lipotoxicity including those leading to formation of excess reactive oxygen (44), creation of endoplasmic reticulum stress (45), development of apoptosis (45, 46), and dysfunction of mitochondria (44). Previous data from our laboratory and others have implicated excess PKC activation as causing heart toxicity (47, 48). It is well known that DAG and ceramide activate PKCs (37, 49–51). In the current experiments, increased PKCα activation correlated with DAG and ceramide levels and reduced heart function and its correction. In the heart, chronic PKC activation leads to reduced heart function (52) and is likely to be a contributor to the dysfunction found in *hDgat1*$^{-/-}$ mice.

Currently there is much debate about the lipid species that are "toxic" (2). This is especially the case for ceramides. Our observation of increased ceramides in the setting of heart failure provides further evidence linking excessive DAG and ceramides with cardiac lipotoxicity.

TABLE 5
Gene expression in hearts from 4-month-old vehicle- and DGAT1 inhibitor-treated hDgat1$^{-/-}$ mice ($n = 4$)

	hDgat1$^{-/-}$ + placebo	*hDgat1*$^{-/-}$ + inhibitor
Bnp	100 ± 67	176 ± 48
Ppara	100 ± 8	76 ± 11[a]
Ppard	100 ± 15	108 ± 8
Pparg	100 ± 5	101 ± 1
Plin2	100 ± 3	119 ± 7[a]
Plin5	100 ± 19	86 ± 15
Cidec	100 ± 14	102 ± 31
Atgl	100 ± 9	79 ± 6
Cpt1b	100 ± 12	80 ± 17
Aox	100 ± 12	92 ± 27
Cd36	100 ± 4	73 ± 9[a]
Lpl	100 ± 4	107 ± 21
Angptl4	100 ± 36	198 ± 40[a]
Pdk4	100 ± 53	189 ± 95
Glut4	100 ± 20	67 ± 12[a]

[a] $p < 0.05$.

It should be noted that therapy with long acting GLP-1 receptor agonists has a number of pharmacologic actions that could improve heart function, many of which are exclusive of changes in lipid metabolism. In *ex vivo* models, GLP-1 treatment reduced ischemia/reperfusion injury (53), an effect that might be attributed to a shift from fatty acid to glucose oxidation. Increased glucose and reduced fatty acid oxidation reduce ischemic injury presumably due to a reduced requirement for oxygen generation of ATP in the setting of decreased blood flow (54). GLP-1 receptor agonists mediate these beneficial effects even in mice with a cardiomyocyte knock-out of the GLP-1 receptor (43). GLP-1 receptor agonists might have off-target effects, or these drugs could affect cells in the heart other than cardiomyocytes. Specifically, they have been shown to improve survival of endothelial cells after ischemic injury (53).

The heart has both the greatest caloric need and the most robust oxidation of fatty acids. Under pathological conditions such as obesity and type 2 diabetes, cardiac fatty acid uptake and oxidation are not balanced, and hearts accumulate lipids, potentially leading to cardiac lipotoxicity (2). Severe heart failure associated with a marked reduction in fatty acid oxidation also leads to accumulation of DAG and ceramides (9). This is associated with a marked decrease in DGAT1 expression. Our mouse studies show that these changes in lipid metabolism alone can alter heart function. Moreover, interventions that reduce cardiac lipid uptake appear to rebalance heart lipid metabolism, reduce PKC activation, and improve heart function. Other conditions such as the heart dysfunction that occurs with metabolic syndrome, type 2 diabetes, and myocardial infarction may also be improved by approaches that prevent abnormal cardiac accumulation of undesirable lipids.

REFERENCES

1. Unger, R. H., and Scherer, P. E. (2010) Gluttony, sloth and the metabolic syndrome: a roadmap to lipotoxicity. *Trends Endocrinol. Metab.* **21,** 345–352
2. Goldberg, I. J., Trent, C. M., and Schulze, P. C. (2012) Lipid metabolism and toxicity in the heart. *Cell Metab.* **15,** 805–812
3. Szczepaniak, L. S., Dobbins, R. L., Metzger, G. J., Sartoni-D'Ambrosia, G., Arbique, D., Vongpatanasin, W., Unger, R., and Victor, R. G. (2003) Myocardial triglycerides and systolic function in humans: *in vivo* evaluation by localized proton spectroscopy and cardiac imaging. *Magn. Reson. Med.* **49,** 417–423
4. Szczepaniak, L. S., Victor, R. G., Orci, L., and Unger, R. H. (2007) Forgotten but not gone: the rediscovery of fatty heart, the most common unrecognized disease in America. *Circ. Res.* **101,** 759–767
5. Liu, L., Yu, S., Khan, R. S., Homma, S., Schulze, P. C., Blaner, W. S., Yin, Y., and Goldberg, I. J. (2012) Diacylglycerol acyl transferase 1 overexpression detoxifies cardiac lipids in PPARγ transgenic mice. *J. Lipid Res.* **53,** 1482–1492
6. Liu, L., Yu, S., Khan, R. S., Ables, G. P., Bharadwaj, K. G., Hu, Y., Huggins, L. A., Eriksson, J. W., Buckett, L. K., Turnbull, A. V., Ginsberg, H. N., Blaner, W. S., Huang, L. S., and Goldberg, I. J. (2011) DGAT1 deficiency decreases PPAR expression and does not lead to lipotoxicity in cardiac and skeletal muscle. *J. Lipid Res.* **52,** 732–744
7. Liu, L., Shi, X., Bharadwaj, K. G., Ikeda, S., Yamashita, H., Yagyu, H., Schaffer, J. E., Yu, Y. H., and Goldberg, I. J. (2009) DGAT1 expression increases heart triglyceride content but ameliorates lipotoxicity. *J. Biol. Chem.* **284,** 36312–36323
8. Perman, J. C., Boström, P., Lindbom, M., Lidberg, U., StÅhlman, M., Hägg, D., Lindskog, H., Scharin Täng, M., Omerovic, E., Mattsson Hultén, L., Jeppsson, A., Petursson, P., Herlitz, J., Olivecrona, G., Strickland, D. K., Ekroos, K., Olofsson, S. O., and Borén, J. (2011) The VLDL receptor promotes lipotoxicity and increases mortality in mice following an acute myocardial infarction. *J. Clin. Investig.* **121,** 2625–2640
9. Chokshi, A., Drosatos, K., Cheema, F. H., Ji, R., Khawaja, T., Yu, S., Kato, T., Khan, R., Takayama, H., Knöll, R., Milting, H., Chung, C. S., Jorde, U., Naka, Y., Mancini, D. M., Goldberg, I. J., and Schulze, P. C. (2012) Ventricular assist device implantation corrects myocardial lipotoxicity, reverses insulin resistance, and normalizes cardiac metabolism in patients with advanced heart failure. *Circulation* **125,** 2844–2853
10. Yen, C. L., Stone, S. J., Koliwad, S., Harris, C., and Farese, R. V., Jr. (2008) Thematic review series: glycerolipids. DGAT enzymes and triacylglycerol biosynthesis. *J. Lipid Res.* **49,** 2283–2301
11. Cases, S., Smith, S. J., Zheng, Y. W., Myers, H. M., Lear, S. R., Sande, E., Novak, S., Collins, C., Welch, C. B., Lusis, A. J., Erickson, S. K., and Farese, R. V., Jr. (1998) Identification of a gene encoding an acyl CoA:diacylglycerol acyltransferase, a key enzyme in triacylglycerol synthesis. *Proc. Natl. Acad. Sci. U.S.A.* **95,** 13018–13023
12. Yen, C. L., Monetti, M., Burri, B. J., and Farese, R. V., Jr. (2005) The triacylglycerol synthesis enzyme DGAT1 also catalyzes the synthesis of diacylglycerols, waxes, and retinyl esters. *J. Lipid Res.* **46,** 1502–1511
13. Oelkers, P., Behari, A., Cromley, D., Billheimer, J. T., and Sturley, S. L. (1998) Characterization of two human genes encoding acyl coenzyme A:cholesterol acyltransferase-related enzymes. *J. Biol. Chem.* **273,** 26765–26771
14. Smith, S. J., Cases, S., Jensen, D. R., Chen, H. C., Sande, E., Tow, B., Sanan, D. A., Raber, J., Eckel, R. H., and Farese, R. V., Jr. (2000) Obesity resistance and multiple mechanisms of triglyceride synthesis in mice lacking Dgat. *Nat. Genet.* **25,** 87–90
15. Chen, H. C., Smith, S. J., Ladha, Z., Jensen, D. R., Ferreira, L. D., Pulawa, L. K., McGuire, J. G., Pitas, R. E., Eckel, R. H., and Farese, R. V., Jr. (2002) Increased insulin and leptin sensitivity in mice lacking acyl CoA:diacylglycerol acyltransferase 1. *J. Clin. Investig.* **109,** 1049–1055
16. Ables, G. P., Yang, K. J., Vogel, S., Hernandez-Ono, A., Yu, S., Yuen, J. J., Birtles, S., Buckett, L. K., Turnbull, A. V., Goldberg, I. J., Blaner, W. S., Huang, L. S., and Ginsberg, H. N. (2012) Intestinal DGAT1 deficiency reduces postprandial triglyceride and retinyl ester excursions by inhibiting chylomicron secretion and delaying gastric emptying. *J. Lipid Res.* **53,** 2364–2379
17. Birch, A. M., Buckett, L. K., and Turnbull, A. V. (2010) DGAT1 inhibitors as anti-obesity and anti-diabetic agents. *Curr. Opin. Drug Discov. Devel.* **13,** 489–496
18. Birch, A. M., Birtles, S., Buckett, L. K., Kemmitt, P. D., Smith, G. J., Smith, T. J., Turnbull, A. V., and Wang, S. J. (2009) Discovery of a potent, selective, and orally efficacious pyrimidinooxazinyl bicyclooctaneacetic acid diacylglycerol acyltransferase-1 inhibitor. *J. Med. Chem.* **52,** 1558–1568
19. King, A. J., Segreti, J. A., Larson, K. J., Souers, A. J., Kym, P. R., Reilly, R. M., Collins, C. A., Voorbach, M. J., Zhao, G., Mittelstadt, S. W., and Cox, B. F. (2010) *In vivo* efficacy of acyl CoA:diacylglycerol acyltransferase (DGAT) 1 inhibition in rodent models of postprandial hyperlipidemia. *Eur. J. Pharmacol.* **637,** 155–161
20. Yamamoto, T., Yamaguchi, H., Miki, H., Shimada, M., Nakada, Y., Ogino, M., Asano, K., Aoki, K., Tamura, N., Masago, M., and Kato, K. (2010)

Coenzyme A:diacylglycerol acyltransferase 1 inhibitor ameliorates obesity, liver steatosis, and lipid metabolism abnormality in KKAy mice fed high-fat or high-carbohydrate diets. *Eur. J. Pharmacol.* **640,** 243–249
21. Zhao, G., Souers, A. J., Voorbach, M., Falls, H. D., Droz, B., Brodjian, S., Lau, Y. Y., Iyengar, R. R., Gao, J., Judd, A. S., Wagaw, S. H., Ravn, M. M., Engstrom, K. M., Lynch, J. K., Mulhern, M. M., Freeman, J., Dayton, B. D., Wang, X., Grihalde, N., Fry, D., Beno, D. W., Marsh, K. C., Su, Z., Diaz, G. J., Collins, C. A., Sham, H., Reilly, R. M., Brune, M. E., and Kym, P. R. (2008) Validation of diacyl glycerolacyltransferase I as a novel target for the treatment of obesity and dyslipidemia using a potent and selective small molecule inhibitor. *J. Med. Chem.* **51,** 380–383
22. Denison, H., Nilsson, C., Kujacic, M., Löfgren, L., Karlsson, C., Knutsson, M., and Eriksson, J. W. (2013) Proof of mechanism for the DGAT1 inhibitor AZD7687: results from a first-time-in-human single-dose study. *Diabetes Obes. Metab.* **15,** 136–143
23. Jornayvaz, F. R., and Shulman, G. I. (2012) Diacylglycerol activation of protein kinase Cε and hepatic insulin resistance. *Cell Metab.* **15,** 574–584
24. Rotolo, J., Stancevic, B., Zhang, J., Hua, G., Fuller, J., Yin, X., Haimovitz-Friedman, A., Kim, K., Qian, M., Cardó-Vila, M., Fuks, Z., Pasqualini, R., Arap, W., and Kolesnick, R. (2012) Anti-ceramide antibody prevents the radiation gastrointestinal syndrome in mice. *J. Clin. Investig.* **122,** 1786–1790
25. Geraldes, P., and King, G. L. (2010) Activation of protein kinase C isoforms and its impact on diabetic complications. *Circ. Res.* **106,** 1319–1331
26. Agah, R., Frenkel, P. A., French, B. A., Michael, L. H., Overbeek, P. A., and Schneider, M. D. (1997) Gene recombination in postmitotic cells. Targeted expression of Cre recombinase provokes cardiac-restricted, site-specific rearrangement in adult ventricular muscle *in vivo*. *J. Clin. Investig.* **100,** 169–179
27. Villanueva, C. J., Monetti, M., Shih, M., Zhou, P., Watkins, S. M., Bhanot, S., and Farese, R. V., Jr. (2009) Specific role for acyl CoA:diacylglycerol acyltransferase 1 (Dgat1) in hepatic steatosis due to exogenous fatty acids. *Hepatology* **50,** 434–442
28. Liu, L., Zhang, Y., Chen, N., Shi, X., Tsang, B., and Yu, Y. H. (2007) Upregulation of myocellular DGAT1 augments triglyceride synthesis in skeletal muscle and protects against fat-induced insulin resistance. *J. Clin. Investig.* **117,** 1679–1689
29. Folch, J., Lees, M., and Sloane Stanley, G. H. (1957) A simple method for the isolation and purification of total lipides from animal tissues. *J. Biol. Chem.* **226,** 497–509
30. Preiss, J. E., Loomis, C. R., Bell, R. M., and Niedel, J. E. (1987) Quantitative measurement of sn-1,2-diacylglycerols. *Methods Enzymol.* **141,** 294–300
31. Deleted in proof
32. Deleted in proof
33. Lee, B., Fast, A. M., Zhu, J., Cheng, J. X., and Buhman, K. K. (2010) Intestine-specific expression of acyl CoA:diacylglycerol acyltransferase 1 reverses resistance to diet-induced hepatic steatosis and obesity in Dgat1−/− mice. *J. Lipid Res.* **51,** 1770–1780
34. Drosatos, K., Bharadwaj, K. G., Lymperopoulos, A., Ikeda, S., Khan, R., Hu, Y., Agarwal, R., Yu, S., Jiang, H., Steinberg, S. F., Blaner, W. S., Koch, W. J., and Goldberg, I. J. (2011) Cardiomyocyte lipids impair β-adrenergic receptor function via PKC activation. *Am. J. Physiol. Endocrinol. Metab.* **300,** E489–E499
35. Lin, H. V., Chen, D., Shen, Z., Zhu, L., Ouyang, X., Vongs, A., Kan, Y., Levorse, J. M., Kowalik, E. J., Jr., Szeto, D. M., Yao, X., Xiao, J., Chen, S., Liu, J., Garcia-Calvo, M., Shin, M. K., and Pinto, S. (2013) Diacylglycerol acyltransferase-1 (DGAT1) inhibition perturbs postprandial gut hormone release. *PLoS One* **8,** e54480
36. Cao, J., Zhou, Y., Peng, H., Huang, X., Stahler, S., Suri, V., Qadri, A., Gareski, T., Jones, J., Hahm, S., Perreault, M., McKew, J., Shi, M., Xu, X., Tobin, J. F., and Gimeno, R. E. (2011) Targeting acyl-CoA:diacylglycerol acyltransferase 1 (DGAT1) with small molecule inhibitors for the treatment of metabolic diseases. *J. Biol. Chem.* **286,** 41838–41851
37. Dobrzyn, A., Dobrzyn, P., Lee, S. H., Miyazaki, M., Cohen, P., Asilmaz, E., Hardie, D. G., Friedman, J. M., and Ntambi, J. M. (2005) Stearoyl-CoA desaturase-1 deficiency reduces ceramide synthesis by downregulating serine palmitoyltransferase and increasing beta-oxidation in skeletal muscle. *Am. J. Physiol. Endocrinol. Metab.* **288,** E599–E607
38. Morrow, J. P., Katchman, A., Son, N. H., Trent, C. M., Khan, R., Shiomi, T., Huang, H., Amin, V., Lader, J. M., Vasquez, C., Morley, G. E., D'Armiento, J., Homma, S., Goldberg, I. J., and Marx, S. O. (2011) Mice with cardiac overexpression of peroxisome proliferator-activated receptor γ have impaired repolarization and spontaneous fatal ventricular arrhythmias. *Circulation* **124,** 2812–2821
39. Streeper, R. S., Grueter, C. A., Salomonis, N., Cases, S., Levin, M. C., Koliwad, S. K., Zhou, P., Hirschey, M. D., Verdin, E., and Farese, R. V., Jr. (2012) Deficiency of the lipid synthesis enzyme, DGAT1, extends longevity in mice. *Aging* **4,** 13–27
40. Chen, H. C., Ladha, Z., Smith, S. J., and Farese, R. V., Jr. (2003) Analysis of energy expenditure at different ambient temperatures in mice lacking DGAT1. *Am. J. Physiol. Endocrinol. Metab.* **284,** E213–E218
41. Chen, H. C., Jensen, D. R., Myers, H. M., Eckel, R. H., and Farese, R. V., Jr. (2003) Obesity resistance and enhanced glucose metabolism in mice transplanted with white adipose tissue lacking acyl CoA:diacylglycerol acyltransferase 1. *J. Clin. Investig.* **111,** 1715–1722
42. Ussher, J. R., and Drucker, D. J. (2012) Cardiovascular biology of the incretin system. *Endocr. Rev.* **33,** 187–215
43. Ussher, J. R., Baggio, L. L., Campbell, J. E., Mulvihill, E. E., Kim, M., Kabir, M. G., Cao, X., Baranek, B. M., Stoffers, D. A., Seeley, R. J., and Drucker, D. J. (2014) Inactivation of the cardiomyocyte glucagon-like peptide-1 receptor (GLP-1R) unmasks cardiomyocyte-independent GLP-1R-mediated cardioprotection. *Mol. Metab.* **3,** 507–517
44. Vamecq, J., Dessein, A. F., Fontaine, M., Briand, G., Porchet, N., Latruffe, N., Andreolotti, P., and Cherkaoui-Malki, M. (2012) Mitochondrial dysfunction and lipid homeostasis. *Curr. Drug Metab.* **13,** 1388–1400
45. Pineau, L., and Ferreira, T. (2010) Lipid-induced ER stress in yeast and β cells: parallel trails to a common fate. *FEMS Yeast Res.* **10,** 1035–1045
46. Unger, R. H. (2002) Lipotoxic diseases. *Annu. Rev. Med.* **53,** 319–336
47. Braz, J. C., Gregory, K., Pathak, A., Zhao, W., Sahin, B., Klevitsky, R., Kimball, T. F., Lorenz, J. N., Nairn, A. C., Liggett, S. B., Bodi, I., Wang, S., Schwartz, A., Lakatta, E. G., DePaoli-Roach, A. A., Robbins, J., Hewett, T. E., Bibb, J. A., Westfall, M. V., Kranias, E. G., and Molkentin, J. D. (2004) PKC-α regulates cardiac contractility and propensity toward heart failure. *Nat. Med.* **10,** 248–254
48. Hahn, H. S., Marreez, Y., Odley, A., Sterbling, A., Yussman, M. G., Hilty, K. C., Bodi, I., Liggett, S. B., Schwartz, A., and Dorn, G. W., 2nd (2003) Protein kinase Cα negatively regulates systolic and diastolic function in pathological hypertrophy. *Circ. Res.* **93,** 1111–1119
49. Newton, A. C. (2009) Lipid activation of protein kinases. *J. Lipid Res.* **50,** (suppl.) S266–S271
50. Idris, I., and Donnelly, R. (2006) Protein kinase Cβ inhibition: a novel therapeutic strategy for diabetic microangiopathy. *Diab. Vasc. Dis. Res.* **3,** 172–178
51. Schmitz-Peiffer, C. (2000) Signalling aspects of insulin resistance in skeletal muscle: mechanisms induced by lipid oversupply. *Cell. Signal.* **12,** 583–594
52. Liu, Q., and Molkentin, J. D. (2011) Protein kinase Cα as a heart failure therapeutic target. *J. Mol. Cell. Cardiol.* **51,** 474–478
53. Noyan-Ashraf, M. H., Shikatani, E. A., Schuiki, I., Mukovozov, I., Wu, J., Li, R. K., Volchuk, A., Robinson, L. A., Billia, F., Drucker, D. J., and Husain, M. (2013) A glucagon-like peptide-1 analog reverses the molecular pathology and cardiac dysfunction of a mouse model of obesity. *Circulation* **127,** 74–85
54. Axelsen, L. N., Keung, W., Pedersen, H. D., Meier, E., Riber, D., Kjølbye, A. L., Petersen, J. S., Proctor, S. D., Holstein-Rathlou, N. H., and Lopaschuk, G. D. (2012) Glucagon and a glucagon-GLP-1 dual-agonist increases cardiac performance with different metabolic effects in insulin-resistant hearts. *Br. J. Pharmacol.* **165,** 2736–2748